REPORT DOCUMENTATION PAGE

Form Approved
OMB No. 0704-0188

PLEASE DO NOT RETURN YOUR FORM TO THE ABOVE ORGANIZATION.

1. REPORT DATE *(DD-MM-YYYY)*	2. REPORT TYPE	3. DATES COVERED *(From - To)*
20-12-2017	Final	09 June 2014 – 08 June 2017

4. TITLE AND SUBTITLE
Exploitation of Infrared Radiance and Retrieval Product Data to Improve Numerical Dust Modeling

5a. CONTRACT NUMBER

5b. GRANT NUMBER
N00173-14-1-G905

5c. PROGRAM ELEMENT NUMBER

6. AUTHOR(S)
Robert Holz (PI)

5d. PROJECT NUMBER
75-036C-16

5e. TASK NUMBER

5f. WORK UNIT NUMBER

7. PERFORMING ORGANIZATION NAME(S) AND ADDRESS(ES)
University of Wisconsin
1015 Atmospheric Oceanic & Space Sciences
1225 Dayton Street
Madison, WI 53706

8. PERFORMING ORGANIZATION REPORT NUMBER

9. SPONSORING/MONITORING AGENCY NAME(S) AND ADDRESS(ES)
Office of Naval Research
230 South Dearborn, Room 380
Chicago, IL 60604-1595

10. SPONSOR/MONITOR'S ACRONYM(S)
ONR

11. SPONSOR/MONITOR'S REPORT NUMBER(S)

12. DISTRIBUTION/AVAILABILITY STATEMENT
Approved for Public Release; Distribution is Unlimited

13. SUPPLEMENTARY NOTES

14. ABSTRACT
This is the final report for ONR grant N00173-14-1-G905 which focused on developing IR dust detection and Aerosol Optical Thickness retrievals applied to hyperspectral infrared observations. This research focused on UAV Global Hawk flights in the eastern Atlantic Ocean as part the NASA HS3 mission providing well calibrated collocated hyper-spectral IR data with coincident lidar (Cloud Physics Lidar CPL) data in addition to frequent drop sound measurements during the flights. This combination provides a unique, well constrained data set to investigate the information content of dust in the IR validated with the lidar profiles.

15. SUBJECT TERMS
Dust
IR retrievals
Aerosols

16. SECURITY CLASSIFICATION OF:			17. LIMITATION OF ABSTRACT	18. NUMBER OF PAGES	19a. NAME OF RESPONSIBLE PERSON
a. REPORT	b. ABSTRACT	c. THIS PAGE			Robert Holz
u	u	u	uu	14	19b. TELEPHONE NUMBER *(Include area code)* 608 263 7254

Reset

Final Report Grant: N00173-14-1-G905

1. INTRODUCTION

This is the final report for ONR grant N00173-14-1-G905 which focused on developing IR dust detection and Aerosol Optical Thickness retrievals applied to hyperspectral infrared observations. This research focused on UAV Global Hawk flights in the eastern Atlantic Ocean as part the NASA HS3 mission providing well calibrated collocated hyper-spectral IR data with coincident lidar (Cloud Physics Lidar CPL) data in addition to frequent drop sound measurements during the flights. This combination provides a unique, well constrained data set to investigate the information content of dust in the IR validated with the lidar profiles.

Mineral dust in particular interacts with both short and longwave radiation directly, and indirectly through ice cloud nucleation (Slingo). Proper characterization of aerosol loading corrects systematic errors in radiance assimilation and increases the accuracy of numerical weather prediction solutions (e.g. Haywood et al., 2005; Perez et al., 2006). Hayward et al. 2005 found biases of -35 Wm-2 in the UK Met Office model for top-of-atmosphere fluxes over Saharan Africa due to neglecting dust influence. Ruescas et al. (2011) found a dust-based bias in assimilated sea surface temperature retrievals, further negatively influencing NWP models incorporating the data into boundary conditions. Dust most directly influences forecast models by reducing errors in satellite retrieved temperature and water vapor profiles, with sensors incorrectly associating cooler aerosol layers as characteristic of the surface (Westphal and Toon, 1991). Dust has been theorized to even influence tropical cyclone development (Karyampudi and Pierce, 2002; Dunion and Velden, 2004, Davidi et al., 2012). Impacts are not limited to near source regions, often crossing oceans and influencing multiple continents, as in the case of anthropogenic pollution from China, fires in Eastern Russia, Central Africa and the Amazon, or dust from Western Africa and China (ref fill, Damoya, arctas, freitas). Should aerosols reach the stratosphere through mixing, volcanic activity, or pyro-convection, all temporal and spatial scales increase, creating global implications for weeks to months (ref {any Fromm, Pinatubo, El Chincon}). The importance of aerosols extends to direct impacts on human society. Poor air quality impedes biological processes increasing acute failures in human cardiovascular and respiratory systems (ref Seaton, Poschl, China autism study?). Reduced visibility produced by increased extinction of visible solar radiation creates hazards for aviation and transportation on land with tephra from volcanoes able to disable aircraft engines. The eruption of Eyjafjallajökull in 2010 resulted in the shutdown of European airspace, affecting over ten million travellers. Not all effects are negative; many Pacific Islands west of the Andesite Line and in the Amazon rainforests rely on trans-oceanic mineral transport for soil fertility (ref...J. Diamond?). Commercially, electrial power grids with contributions from solar energy require forecasts to assess potential shortfalls caused by reduced insolation (Schroedter-Homscheidt et al. 2013).

Despite all this, aerosols also remain one of the most poorly constrained constituents of the environmental system. This is due in part to the discrete nature of aerosol sources and sinks. While aerosols such as dust and sea salts can be reliably predicted (at least near source) using surface meteorology, fires are less foreseeable. Once airborne, removal by precipitation must also be accurately predicted. Limitations in our ability to predict and represent these sources and

sinks require daily, global observations. Polar orbiting satellites provide the best platform for the current generation of global aerosol observations. Sensors such as the Moderate Resolution Imaging SPectro-radiometer (MODIS) and the Multi-angle Imaging SpectroRadiometer (MISR) retrieve total column aerosol information in the visible and near-infrared spectrums, highlighting a major issue: large portions of polar orbital swaths become useless for passive sensors as they transit across the nighttime side of the planet. Nighttime infrared aerosol retrievals have been attempted before using multispectral sensors. Ackerman et al., (1997) developed a scheme using MODIS, however they were unable to sufficiently characterize dust in the limited infrared channels. The key limitation of MODIS in regard to dust is that the signal in the infrared gets washed out by the size of the IR channels. [[Merchant et al. (2006) produced]]. Peyridieu et al. (2010) developed a look-up table approach to using the hyperspectral AIRS data based upon the Thermodynamic Initial Guess Retrieval (TIGR, Chedin et al., 1986) which produced a reasonable agreement with MODIS and CALIOP retrievals. The current suite of available hyperspectral imagers in orbit includes CrIS, IASI, AIRS, and SCHEMACHY, none of which have been fully leveraged to address an infrared aerosol retrieval. Further, validation has not been performed to account for potential mineral dust effects on sounder signals (Nalli and Stow, 2002).

While there are a number of hyperspectral sensors currently in space, our initial development efforts herein are focused on aircraft based platforms. The Scanning High-resolution Interferometer Sounder (S-HIS; ref) flown with the Cloud Physics Lidar (CPL; McGill et al. 2002) provides a unique, collocated dataset. The CPL already provides high resolution vertical information and total column aerosol optical properties, but has a narrow scan width. Like space-based sounders, S-HIS provides the spatial coverage lacking from lidar systems. CPL provides a bootstrapping method of verifying nadir S-HIS scans.

This investigation used spectrally resolved nadir infrared radiance data to determine optical depth of dust layers and quantify information content within a hyperspectral sounder signal. We follow the work of Turner (2008) in which a similar technique is used to determine aerosol properties from up looking hyper-spectral observations. Retrieving aerosol radiative properties from down looking aircraft and satellite observations introduces additional challenges as the retrievals are highly sensitive to the surface properties (emissivity and temperature). To reduce this surface variability, only over-ocean retrievals are currently attempted. The type of mineral constituting mineral dust layers also affects the radiance signature. Source region and the process by which minerals become lifted change the make-up. Glaccum and Prospero (1980) showed that muscovite and illites dominated layers over the Tropical Atlantic while quartz and feldspar were more significant in Morocco and West Africa (Kandler et al. 2009), however sedimentation reduces their relative influence over the Atlantic. Kaolinite and gypsum constitute significant portions of dust over Africa and have unique absorption signatures within the S-HIS spectral range (fig. dBvT). This will introduce the limitation of neglecting less-spectrally significant constituents as well as those spectrally similar.

2. INSTRUMENTATION

S-HIS was developed and is maintained and operated by the Space Science and Engineering Center (SSEC) at the University of Wisconsin-Madison. S-HIS measures upwelling, cross-track radiances between 3.3 and 18 um on high-altitude aircraft including the Global Hawk unmanned aircraft and the NASA ER-2. For the purposes of this study, only data collected from the Global Hawk during the multi-year Hurricane and Severe Storm Sentinel (HS3) mission will be used. At an average aircraft altitude of 20 km (compared to 705 km for many polar satellites), the interferometer has a 2 km spatial resolution at nadir within a 40 km surface swath, with approximately 94% of that atmospheric mass below. S-HIS is a Fourier-transform interferometer (FTIR) device, calibrated to within 0.2 K brightness temperatures for the majority of the spectral range. The unit houses two onboard calibration sources, scanned after each pass through earth fields of view, with one blackbody at ambient temperature and the "hot" blackbody heated up to 60 K above ambient.

The NASA-EOS CPL is an atmospheric lidar that uses solid state photon collectors to provide backscatter profiles at a 30 m vertical resolution for three laser channels at 355 nm, 532 nm, and 1064 nm. Cloud and aerosol properties are derived from these channels. Aerosol optical properties are collected for all channels with the signal being completely attenuated at optical depths of ~3. CPL (and most lidars) suffer from an assumption of only measuring single-scattered particles. This assumption induces errors in retrieved backscatter and optical properties. Reducing the sensor field-of-view size plays the biggest role in limiting multiple scattering signal from thick features. The CPL 100-urad view permits multiple scattering signals up to 15%.

The complexity of the CPL scenes dictates the degree of automation to the process. Part of our goal is to remove such requirements. The data from S-HIS and CPL are complimentary. The CPL has a high vertical resolution but a limited horizontal footprint. It therefore provides a verification source limited to nadir scans of S-HIS, but could be applied to successful development of a retrieval describing total column aerosol characteristics along the entire cross-track swath. We focus on the HS3 missions in particular as, at the time of this writing, these data benefit from the greatest noise filtering and operational quality of any S-HIS deployments. Flights occurred during August and September of 2013. HS3 deployment years had ample opportunity to measure aerosols as their active periods unfortunately coincided with a dearth of hurricane activity in the Atlantic basin. Many flight hours ended up sampling off of West Africa collecting through the Saharan Air Layer (SAL). This layer is often coincident, but not necessarily the same, with the transport layer of dust produced by the African Easterly jet during boreal summer. The SAL produces strong humidity gradients that further complicate sounder retrievals.

3. RETRIEVAL ALGORITHM

Our retrieval development follows an optimal estimation framework (Eq. 1; Rodgers 2000, Eq. 5.9) suitable for exploiting the differences between different mineral spectral radiance signatures in the infrared. This solution is found through an iterative process (i), using a forward model (F) to simulate from state (x_i) to measurement space, and minimize differences between simulated ($F(x_i)$) and observed radiances (y). However, the response across the spectrum to changes in

bulk aerosol characteristics such as effective radius and optical depth is non-linear; small changes at low optical depths may bear no relation to the same changes at high optical depths. This non-linearity requires the simulated responses constituting the Jacobian matrix (K_i) to be recalculated for each iteration, increasing computational expense. Properly constraining the *a priori* (x_a) state reduces convergence iterations and state-space distance to an optimal solution. As such, we seek to identify the largest sources of uncertainty in the state and methods to limit them with a single sensor solution. S_a and S_ϵ are the *a priori* state and observing system error covariance matrices.

$$x_{i+1} = x_i + (S_a^{-1} + K_i^T S_\epsilon^{-1} K_i)^{-1} K_i^T S_\epsilon^{-1} [y - F(x_i) + K_i(x_i - x_a)] \qquad \text{Eq. 1}$$

A benefit of the optimal estimation approach is that the uncertainties in the observing system can be identified within the posterior covariance matrix (Masiello et al.). The observing system includes the forward model, the atmospheric profile used within it, the instrument itself, choice of first guess, as well as any other assumptions affecting the information within simulated or observed measurement space. How these uncertainties propagate through the system can be understood through the use of pseudo-observations. Here we use that term to describe fabricated radiances produced using the forward model for wholly known information in measurement space. The sensitivity of the system to errors within the profile can then be identified by using the same forward model to retrieve on these pseudo-obs. Instrument uncertainty is more straightforward. During operation, the heated blackbody is regularly sampled. Error estimation is derived from its deviation from expected blackbody radiances.

Forward model calculations are performed using the LBL-DIS radiative transfer model. LBL-DIS uses high resolution transmission information from atmospheric gases calculated by the Line-by-Line radiative transfer model (LBLRTM) with the discrete ordinates radiative transfer model (DISORT) to handle scattering and produce upwelling radiances. For the pseudo-obs, LBL-DIS output has been convolved to the spectral characteristics of the S-HIS. The full resolution spectrum is never used during the optimal estimation process. Using the full spectrum of the S-HIS measurement space would make the Jacobian matrices computationally prohibitive. Retrieval sensitivity to noise also increases. Choosing representative "microwindow" channels balances necessary information content with operational requirements. LBL-DIS provides a number of predefined channels, of which we use a modified version of microwindow preset 4, removing the channel at the edge of longwave ozone influence and a water vapor channel centered on 850 cm-1. The sensitivity to LBL-RTM to errors in the Global Data Assimilation System (GDAS; Kanamitsu, 1989) from which the input atmospheric profiles are derived, necessitated their removal. GDAS data are interpolated using the nearest neighbor method from the 1deg x 1deg model grid.

The results focus on both on the information content of the S-HIS signal using simulated data, and the performance of the algorithm on real observations of air masses sampled off Africa. The mineral composition of transported Saharan dust in the Tropical Atlantic is dominated by clays (kaolinite and illite) and quartz, with carbonates (e.g., gypsum) making up around 15% by mass (Prospero and Clusser, 1980; Formenti et al. 2008). The large size and settling velocity of quartz

leads to a decreased loading away from African source regions. Inversely, gypsum loading increases through the dissolution process of calcite. Given this, we focus on the LBLDIS single-scattering properties of two minerals, kaolinite and gypsum, which will be assumed to be characteristic of the transported layers. These minerals were chosen for their distinct spectral characteristics in the longwave window channels (Turner...2008, Figure 1). Retrieved properties for each mineral are separately calculated within the Jacobian allowing for independent adjustments, or even removal, to the distribution. In tropical regions, radiative effects of static water cloud layers near 1.5 km are permitted to allow for cloud contaminated retrievals.

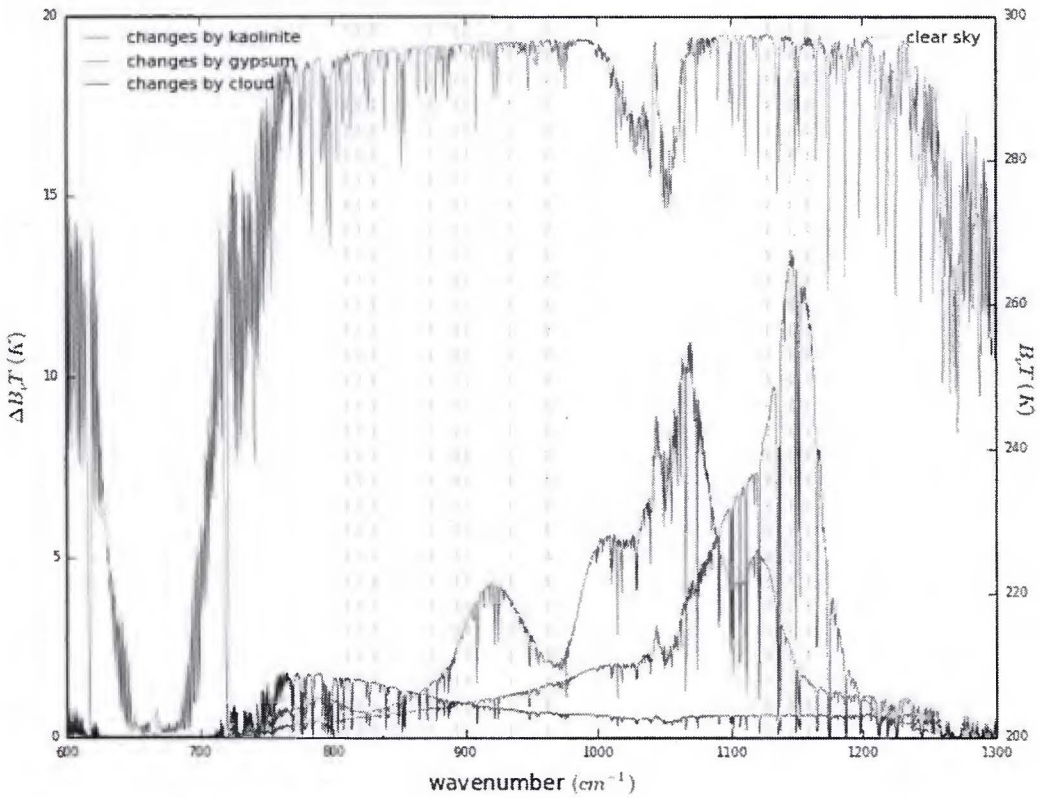

Figure 1. Changes in top of atmosphere brightness temperatures for an optical depth of 1 for the standard tropical atmosphere. Kaolinite, gypsum, and a water cloud in red, green, and blue, respectively. Absolute brightness temperatures for a clear sky case presented in black for reference. Vertical dashes represent all potential micro-window channels used for retrievals. (include water cloud delta line? Darken dashed lines.)

Table 1: Center wavenumber for retrieval micro-window channels (cm-1).

MW#											

26	811.0	819.9	831.8	874.9	893.9	901.8	934.7	962.1			
27	811.0	819.9	831.8	874.9	893.9	901.8	934.7	962.1	1128.5	1145.1	1159.3

4. RESULTS

4.1 SOURCES OF UNCERTAINTY

Pseudo-observations provide information on the limitations of the retrieval. It does so by quantifying the influence of individual error sources and directing constraint efforts. Four thousand obs were generated over a range of heights (1-5 km), optical thicknesses (0.05 - 2.0), and effective radii (0.5 - 30 um), with randomly generated noise similar to that seen in S-HIS operation. Information content within the signal becomes extremely thin for optical thicknesses less than 0.1 (figure UNC. Uncertainty again increases at the other extreme. High optical depths suffer as the transported mineral saturation reduces the information content in the IR. Aerosol layer geometry (thickness and altitude) were the largest sources of error. The spectral similarity of high, thin and low, thick layers is at the core of the inverse problem. To remove the multiple state space solutions, different methods to constrain *a priori* layer geometries are discussed in §4.2.?. Within the range of common optical depths, uncertainty from the instrument and

atmospheric profile estimation error are operationally negligible.

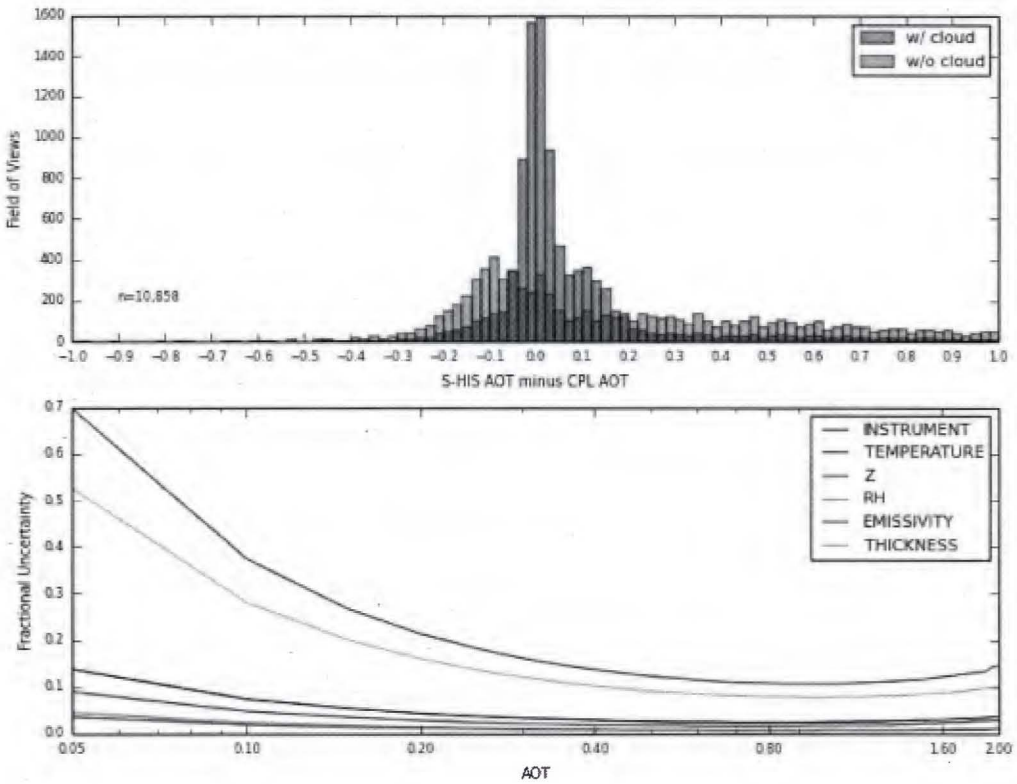

Figure 2: Posterior retrieval uncertainty of pseudo-observation retrievals by source. Uncertainties in the dust layer height (Z) and geometric thickness are the dominant sources of uncertainties in the IR retrieval.

4.1.2 HABIT SENSITIVITY

Pseudo-observations were also used to explore sensitivity to the mineral habit used during the retrieval process. Limited field campaigns and knowledge of source region gives us a starting point to estimate transport layer mineral composition, but we must also understand the types of errors expected when we're wrong. To do this, we again generated pseudo-obs using the spectral properties of kaolinite and gypsum. Retrievals were then limited to using incorrect spectral properties; that is, LBL-DIS given a kaolinite spectral database to retrieve a gypsum layer, and vise versa. Retrievals were performed using channel selections 26 and 27 (table 1) to account for differences in the inclusion of the 1150 cm-1 gypsum peak.

Regardless of channel selection, retrievals using gypsum spectral information produced less error. Inclusion of the gypsum channels actually produces a strong negative bias for lower ODs in the gypsum retrievals (GoK; Fig. HAB_0). Kaolinite retrievals (KoG) consistently over-estimated thicknesses. This occurs when the optimal estimation process, unable to match the

character of gypsum, attempts to bisect the kaolinite peak (900 cm-1) with the linear gypsum signature. This can be seen in the first and third panels of figure HAB_1. A similar bisection happens during the gypsum retrievals, but required less extreme optical thicknesses.

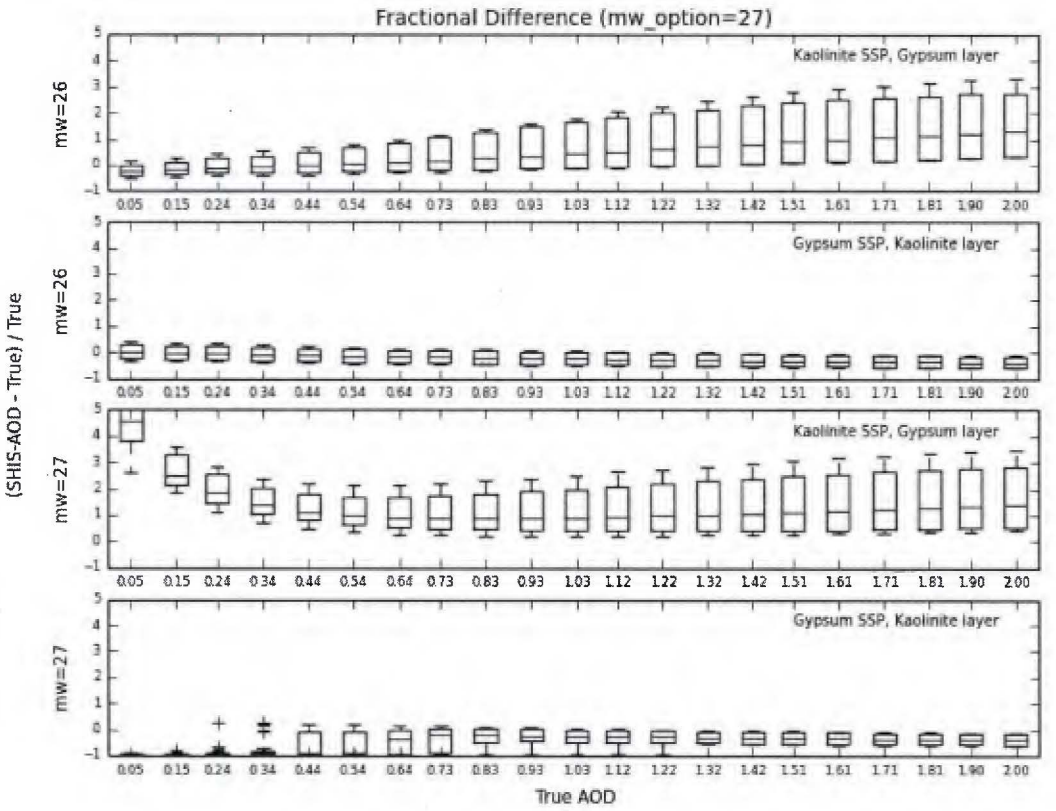

Figure 3: Fractional difference between retrieved AOD and true AOD. Which mineral habit used to generate the pseudo-observations and the habit used in the retrievals are indicated as text. Microwindow options are indicated along y-axis, referencing Table 1.

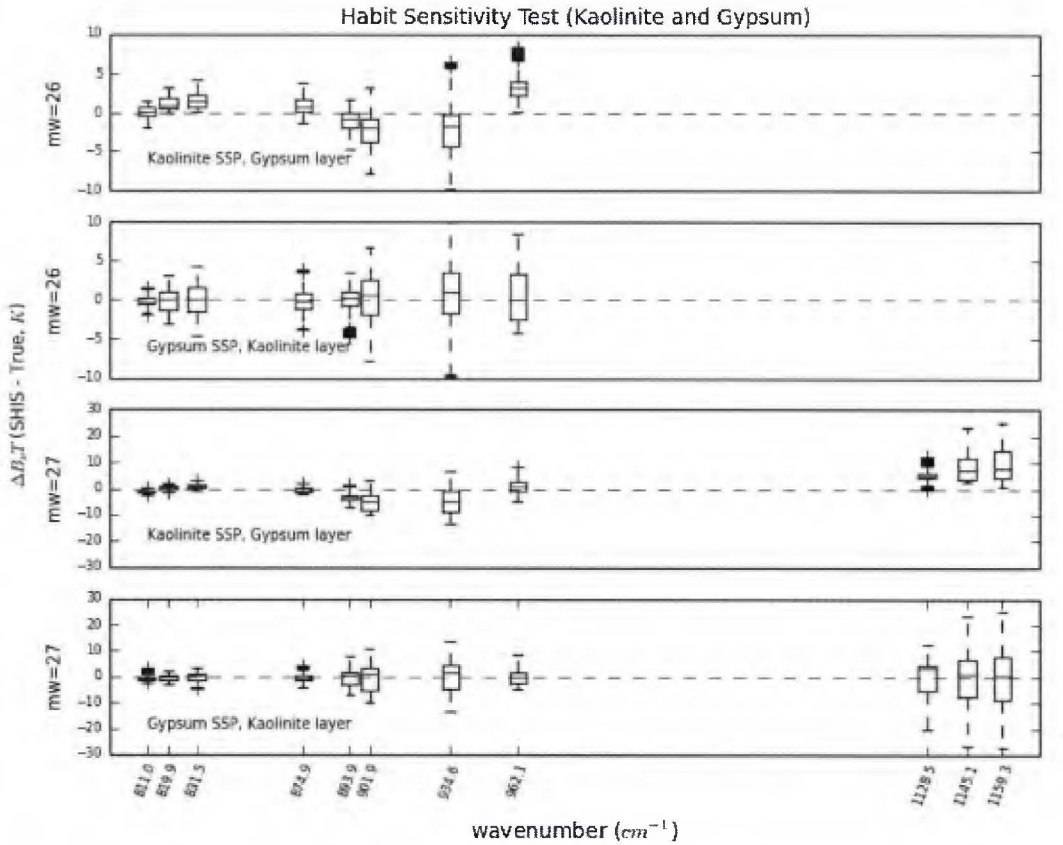

Figure 4: Difference between brightness temperatures between retrieval and pseudo-observation data at microwindow selections 26 and 27 (see Table 1).

4.2.1 TEST CASE DESCRIPTIONS

Several iterations of the retrieval process were run on HS3 campaign radiances to explore the optimal configuration of *a priori* and system parameterizations. The simulated uncertainty above drives much of our focus here. The retrieval requires *a priori* estimates of the aerosol layer; given the importance of layer geometry seen above, constraining it is paramount. Static values for layer top height (1, 3, 5 km) as well as derived layer height products from 72 hour dust forecast values are tested as suitable first guesses. Forecast values are provided by the Navy Aerosol Analysis and Prediction System (NAAPS), the US Navy's offline chemical transport model running with dust, smoke, sulfate and sea salt at 1◦×1 ◦ /27 vertical levels based on the Danish Eulerian Hemispheric Model (Christensen, 1997; Witek et al., 2007; Westphal et al. 2009). High cirrus clouds present a challenge for the dust retrievals across the spectrum and affected scenes were filtered out using the CPL. Low clouds create a different problem; often mixed at or below the dust loading level, water clouds can be difficult to distinguish from aerosol layers at low levels. Tests were performed permitting the presence of a low water cloud layer, effectively producing a

cloud mask as a byproduct of the optimal estimation process on S-HIS radiances. Comparison of the performance between CPL and S-HIS cloud identification where investigated with the hyper-spectral IR observations demonstrating promise in separating dust from liquid water cloud. Selection of retrieval microwindow channels within LBLDIS also varies between tests. The 800 - 970 cm-1 channels focus on kaolinite sensitivity outside of the 1000 cm-1 ozone region (fig. lwT), while the 1100 - 1200 cm-1 channels lie within the primary gypsum peak. Inclusion of the latter in initial tests presented issues discussed below, resulting in cases with and without them being utilized for the retrieval. Many LBLDIS preset channel options contained one centered at 857 cm-1 coincident with enhanced water vapor absorption (fig. lwT) that we removed to reduce sensitivity to potential GDAS water vapor errors.

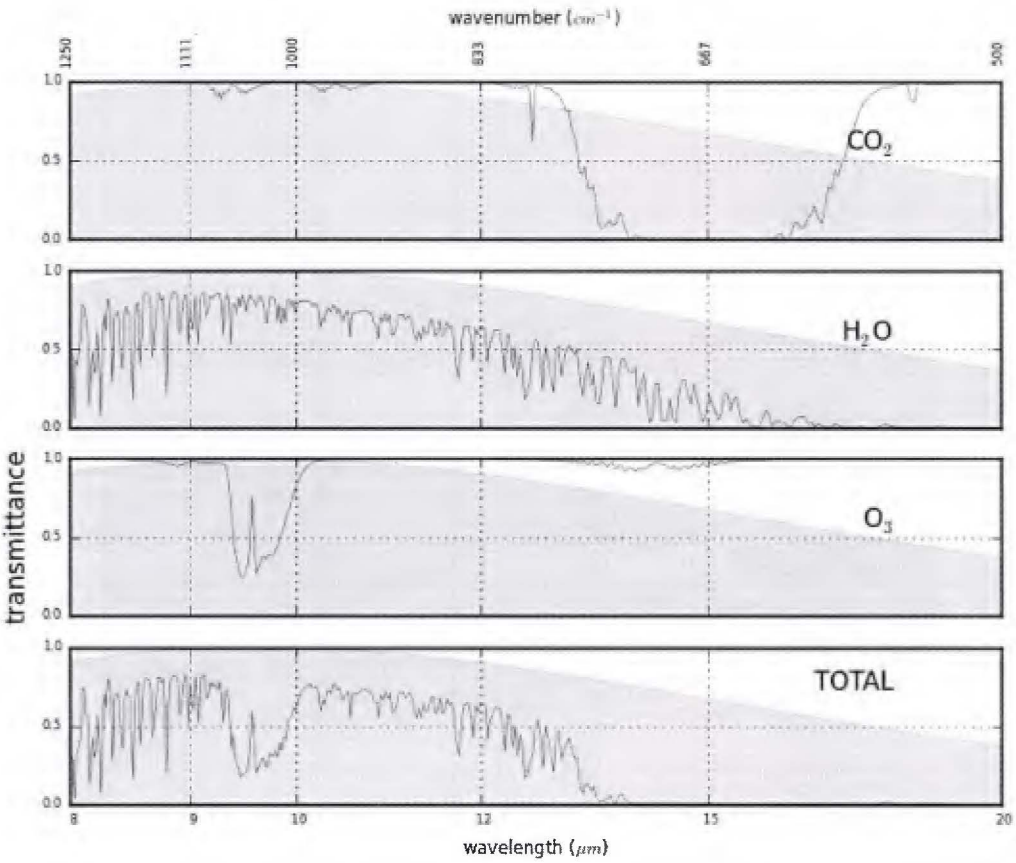

Figure 5: Atmospheric transmittance within the longwave spectrum for carbon dioxide, water vapor, and ozone. Shaded regions represents Planck function at 300 K in wavelength space. Influence of methane can be observed in total near 8 um, but is negligible for our study.

Retrievals were obtained over all collocated S-HIS/CPL field of views for the HS3 2013 science flights. Transit flights and overland scenes were ignored. We present a brief description of characteristic features in figure CPL, which shows that during the campaign, both elevated and near surface aerosol events are present in the 532 nm backscatter channel. CPL aerosol optical thicknesses are noisy throughout these features. Dust layers above low level clouds, such as

during 29 August flight, produced potentially spurious CPL thicknesses exceeding 2 sporadically throughout the layer. Long cloud sections seen in the 9 September backscatter shows one of the few tropical depressions observed. The Central African fire and North African dust transport seasons peaking in boreal summer and spring respectively. Flight tracks would be directly influenced by the easterly African jet transport. Equatorial African smoke requires the high pressure over the Atlas mountains to draw biomass burning emissions northward. This does not appear to happen during the science flight period (Figure NAOD). A NAAPS climatology (including assimilated MODIS and MISR aerosol data; Reid) shows only two flights intersecting smoke during transit legs, with mineral dust from Africa dominating the sampling.

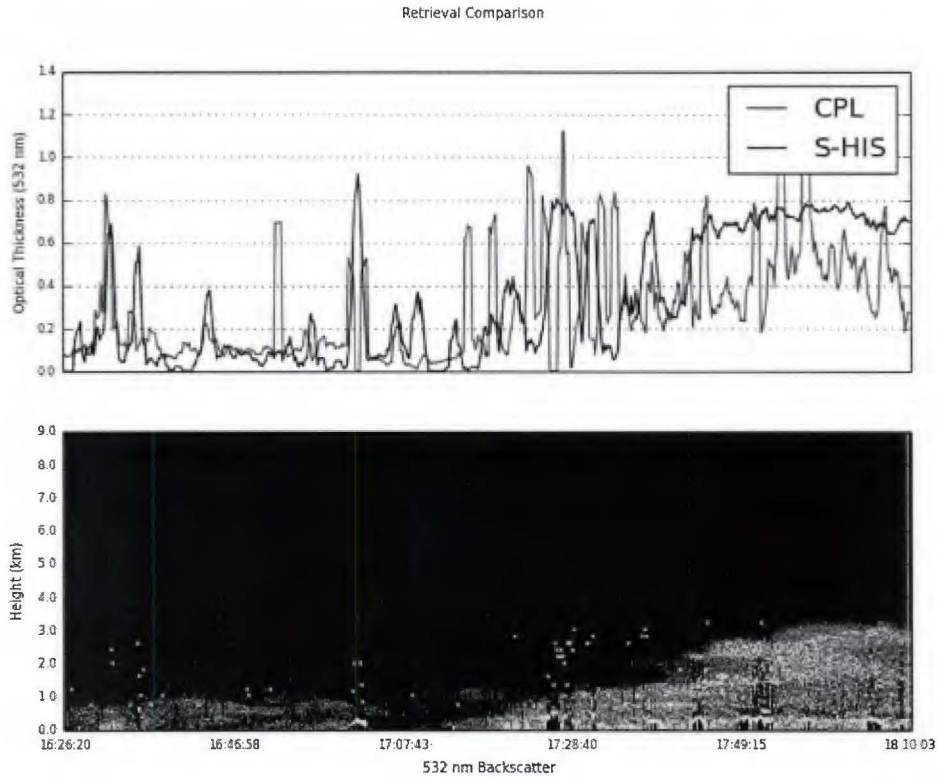

Figure 8 A case study using OE AOT retrieval applied to S-HIS nadir FOV is presented on the top figure. There is reasonable agreement with the collocated CPL retrieved total column AOT (red line). The CPL requires assumption regarding the dust lidar ratio and as a result likely has significant uncertainties with regards to absolute AOT however we the relative changes should be well resolved. The bottom figure presents the CPL attenuated backscatter profile providing the vertical structure of the dust layers retrieved in the top

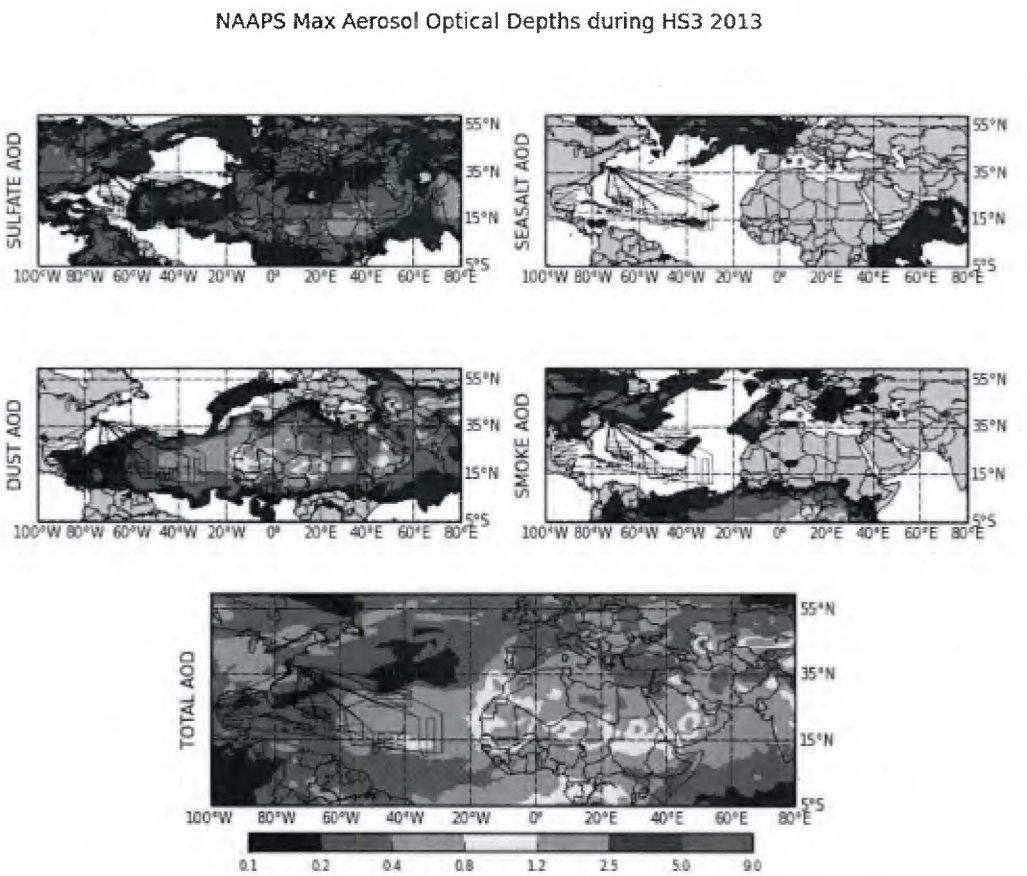

Figure 6: Maximum 550 nm optical depths from four model aerosol species (primary sulfates, sea salt, dust, smoke) and total from NAAPS climatological data, which includes MODIS and MISR data. Flight tracks for HS3 2013 are overlaid.

4.2.2 CLEAR SKY BIAS

The nature of our radiance retrieval relies on dust producing signal bias and this bias must be quantifiable within the forward model. Before attempting a retrieval using the forward model, any systematic bias resulting from either the model or the inputs must be assessed. To do so, we manually filtered through all collocated fields of view for S-HIS and CPL to find scenes showing minimal influence of aerosol or cloud layers. Automated filter techniques failed as both S-HIS and CPL layer algorithms would flag contaminated scenes as clear and vice versa. A slight positive bias can be observed when comparing the observed clear sky radiances from the S-HIS and LBLDIS (fig. BIAS). The bias was most pronounced in the 847 cm-1 and > 1100 channels, indicating errors in the GDAS water vapor profile. The overall bias remains within +/- 1 K throughout the spectrum.

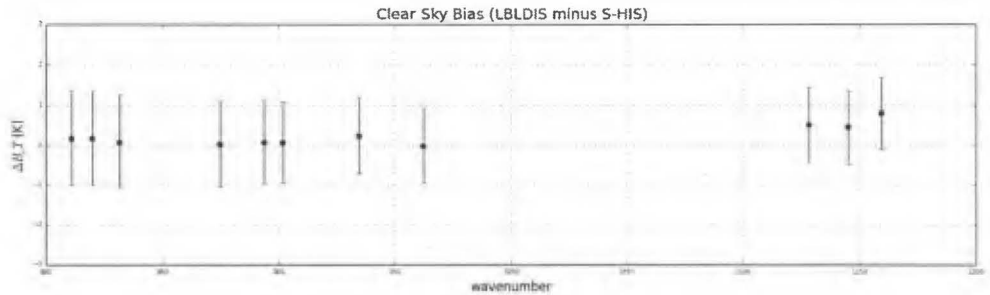

Figure 7: Difference between LBLDIS and S-HIS observed brightness temperatures for clear sky cases during HS3 2013. (Replot: Do over full channels, overlay transmission, make size appropriate to information content)